

Diversity of TiO₂: Controlling the Molecular and Electronic Structure of Atomic-Layer-Deposited Black TiO₂

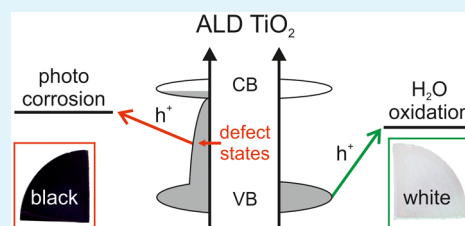
Harri Ali-Löytty,^{*,†} Markku Hannula,[†] Jesse Saari,[†] Lauri Palmolahti,[†] Bela D. Bhuskute,[†] Riina Ulkuniemi,[†] Tuomo Nyysönen,[‡] Kimmo Lahtonen,[†] and Mika Valden[†]

[†]Surface Science Group, Laboratory of Photonics, and [‡]Metals Technology Group, Laboratory of Materials Science, Tampere University of Technology, Tampere FI-33101, Finland

Supporting Information

ABSTRACT: Visually black, electrically leaky, amorphous titania (am-TiO₂) thin films were grown by atomic layer deposition (ALD) for photocatalytic applications. Broad spectral absorbance in the visible range and exceptional conductivity are attributed to trapped Ti³⁺ in the film. Oxidation of Ti³⁺ upon heat treatment leads to a drop in conductivity, a color change from black to white, and crystallization of am-TiO₂. ALD-grown black TiO₂, without any heat treatment, is subject to dissolution in alkaline photoelectrochemical conditions. The best photocatalytic activity for solar water splitting is obtained for completely crystalline white TiO₂.

KEYWORDS: atomic layer deposition, titanium dioxide, oxide defects, crystallization, protecting overlayers, photocatalysis, water splitting



Black titania (TiO₂) is a promising material for providing increased photocatalytic efficiency due to its pronounced solar absorption compared to conventional white or transparent, nonconductive TiO₂ with large bandgap (3.0–3.2 eV) which is capable of absorbing light only in the UV range.¹ Black TiO₂ is often synthesized from white TiO₂ via treatment in a reductive H₂ atmosphere that introduces disorder via oxide defects or H dopants into the TiO₂ structure.^{1–4} On the other hand, transparent amorphous TiO₂ (am-TiO₂) thin film grown by atomic layer deposition (ALD) has shown exceptional charge transfer properties and is therefore utilized as a protection layer for unstable semiconductor materials in photoelectrochemical (PEC) applications.⁵ However, the stability of ALD grown am-TiO₂ under PEC conditions has remained controversial, since most studies have involved an additional catalyst overlayer on am-TiO₂.⁶ Recent work by Yu et al.⁷ revealed a metastable intermediate within an ALD grown am-TiO₂ thin film on Si photoanode that induced corrosion, despite the additional Ni overlayer. We have shown that bare ALD grown am-TiO₂ is subject to rapid photo-corrosion under PEC conditions.⁸ Even crystalline TiO₂ that is believed to be extremely stable, has been shown to suffer from photohole induced corrosion under PEC conditions.⁹ There is an urgent need for better understanding of the TiO₂ corrosion mechanism to be able to develop TiO₂-based materials for photocatalytic energy conversion devices. Here we report a direct synthesis of black TiO₂ by ALD and address the question of inherent stability of ALD-grown electrically leaky titania.

ALD of TiO₂ was carried out at 200 °C in a commercial ALD reactor using tetrakis(dimethylamido)titanium(IV) (TDMAT) and water as precursors and Ar as carrier/purge/

venting gas.⁸ N-type Si(100) wafer was used as a substrate with the exceptions of optical and electrical measurements for which a transparent quartz (SiO₂) glass was used as a substrate. The TiO₂ film thickness of 30 nm was optimized in terms of PEC efficiency for water oxidation, and thus chosen for detailed analysis.

Figure 1 shows the UV–vis absorption results of ALD TiO₂ after deposition and after annealing in oxidizing (air) and reducing (UHV) conditions. The oxidized sample depicts characteristic absorption behavior of rutile TiO₂ with absorption edge at 387 nm (3.2 eV) and no absorption in the visible range. In contrast, the absorption edge for the as-deposited TiO₂ was observed at 344 nm (3.6 eV), which is strongly blue-shifted from the absorption edge of rutile TiO₂ and the absorption edge is followed by a broad absorption that gives rise to the black color of the TiO₂ film.

The increased absorption below the band gap energy is characteristic to free charge carrier absorption or absorption due to intraband gap states. The broad absorption of the as-deposited sample following approximately a logarithmic trend from 350 to 800 nm suggests trapped charge carriers within the band gap, which are assigned later to Ti³⁺.¹⁰ This is supported by the blue-shift in absorption edge compared to rutile TiO₂ which we interpret as the Moss–Burstein effect¹¹ due to the excess population of the conduction band. Interestingly, annealing under reductive conditions induced a clear decrease in the absorption at 528 nm that corresponds to the absorption of trapped holes in TiO₂.¹² Recently, we showed that the same

Received: November 23, 2018

Accepted: January 4, 2019

Published: January 4, 2019

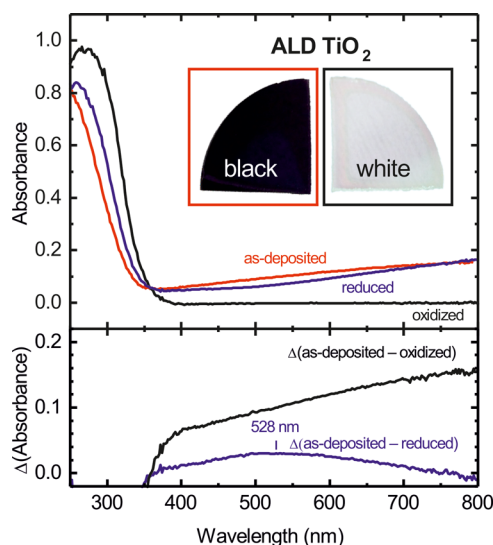


Figure 1. Absorbance of a 30 nm thick black TiO₂ film measured after ALD growth (as-deposited), after annealing in air at 500 °C (oxidized) and after annealing in ultrahigh vacuum (UHV) at 600 °C (reduced). The inset shows pictures of 200 nm thick TiO₂ films after deposition (black) and after annealing in air at 500 °C (white). The difference spectra in the bottom presents the change in absorbance induced by the heat treatments.

reductive heat treatment improved the stability of black am-TiO₂ under PEC conditions, which was attributed to the formation of O⁻ species via electron transfer from O to Ti.⁸ The clear change in optical absorption suggests that the electron transfer is accompanied by the recombination of trapped holes.

Oxidation induced changes on the charge carrier distribution were studied in terms of electrical conductivity and optical absorption as shown in Figure 2. The oxidation treatment was carried out under ambient air by placing the sample into a preheated tube furnace for 45 min. In addition to the aforementioned broad absorbance in the Vis range and enlarged bandgap (Figure 2b, Figure S1) black TiO₂ exhibits exceptionally high conductivity of 150 S/m (Figure 2a). A slight change in the properties was observed upon oxidation at 200 °C followed by more dramatic change for increasing temperatures.

The slight change in the TiO₂ film properties after oxidation at 200 °C is reasonable since the ALD growth was performed at the same temperature. The drastic changes in the electrical

and optical properties correlate perfectly with each other and can be explained by the oxidation of the trapped charge carriers that are responsible for the enhanced conductivity and absorption in the Vis range.

Figure 3 shows scanning electron microscope (SEM) images and grazing-incidence X-ray diffraction (GIXRD) patterns for the oxidized samples. The as-deposited black TiO₂ was found to be amorphous followed by gradual crystallization upon oxidation. In addition to rutile, the crystallized films were found to contain some brookite TiO₂, and quite surprisingly, after oxidation at 350 °C a strong anatase peak appeared. X-ray photoelectron spectroscopy (XPS) reveals that nitrogen (1.8 at. %) is segregated onto the surface at 350 °C that coincides with the formation of the anatase phase (Figure 3c inset). This implies that the small ALD residue concentration of nitrogen plays an important role in the phase stabilization of TiO₂ under these oxidative annealing conditions, although complete crystallization into the most stable rutile TiO₂ via less stable anatase TiO₂ is often observed in the annealing treatments of TiO₂.¹³ Furthermore, the nitrogen concentration within the black am-TiO₂ structure is most likely contributing to the broad absorption in a range of 500–900 nm shown in Figure 1 by providing nitrogen induced in-gap states.

SEM images (Figure 3a) reveal that crystallization initiates at 250 °C, which is not yet clear from the GIXRD (Figure 3b). Most importantly, crystallization was found to follow the oxidation of the trapped charge carriers.

The influence of oxidation on the molecular and valence band structure of black TiO₂ was studied with XPS and ultraviolet photoelectron spectroscopy (UPS), respectively. Figure 4 shows photoelectron spectra by comparing the as-deposited and 500 °C oxidized samples. It is evident from the XP survey spectra that the surfaces of ALD grown TiO₂ films are clean with a small concentration of carbon, which is mainly due to impurities from the air exposure, and <0.3 at. % of nitrogen (Figure 4a). The Ti 2p XPS transitions appear as peaks in the binding energy range of 450–480 eV (Figure 4c). The main Ti 2p_{3/2} and Ti 2p_{1/2} peaks at binding energies of 458.8 and 464.5 eV, respectively, are accompanied by well-known charge transfer shakeup satellite peaks 13 eV above the main peaks.¹⁴ These binding energies and satellite peaks are consistent with the Ti⁴⁺ state of the TiO₂. In addition, a clear shoulder at the binding energy of 457.5 eV can be seen in the XP spectrum measured from the as-deposited sample. This peak can be assigned to the Ti³⁺, which can explain the increased absorption in the Vis range¹⁵ and increased conductivity.

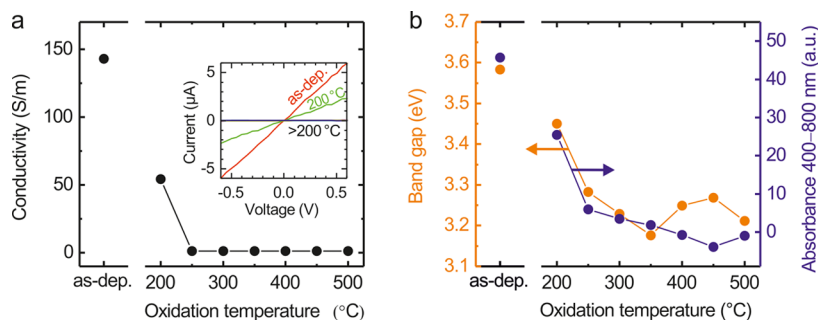


Figure 2. (a) Conductivity and (b) optical band gap and integrated absorbance from 400 to 800 nm for the ALD grown black TiO₂ films after they have been annealed at different oxidation temperatures. Inset in a shows the dramatic change of the *I*–*V* characteristics for the as-deposited TiO₂ film and the TiO₂ films after oxidation treatment at 200 °C and higher temperatures.

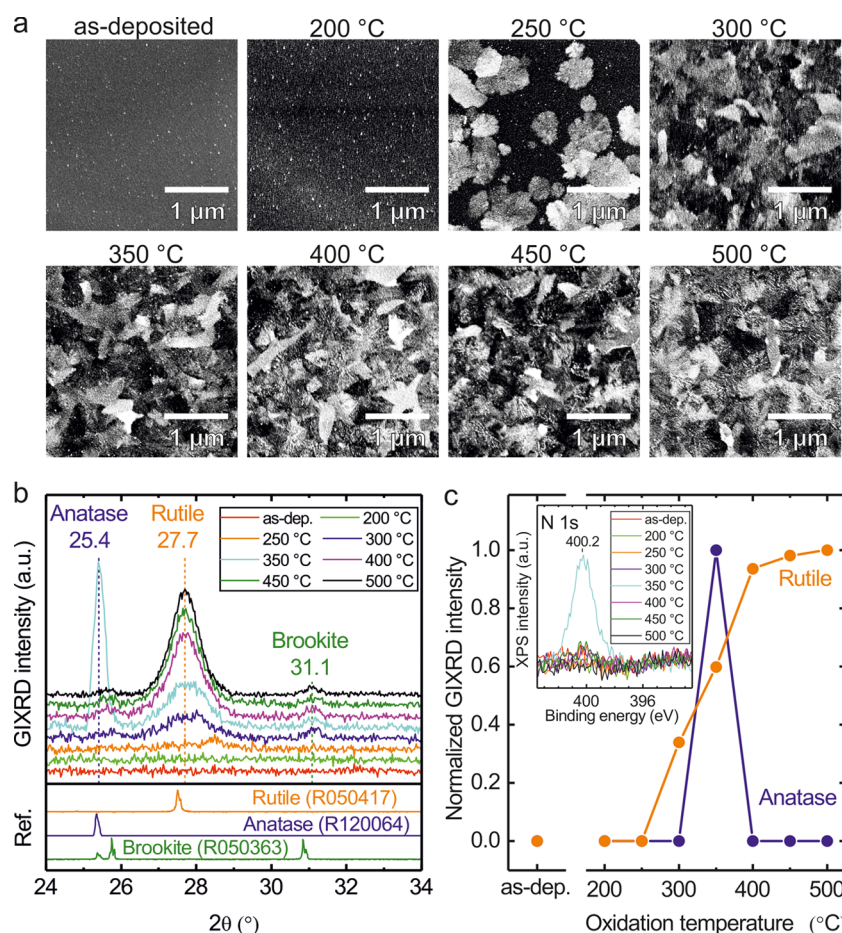


Figure 3. (a) SEM images, (b) GIXRD patterns, and (c) normalized GIXRD intensities of the anatase and rutile peaks for the ALD-grown black TiO₂ films at different oxidation temperatures. Inset in c shows XP spectra of N 1s.

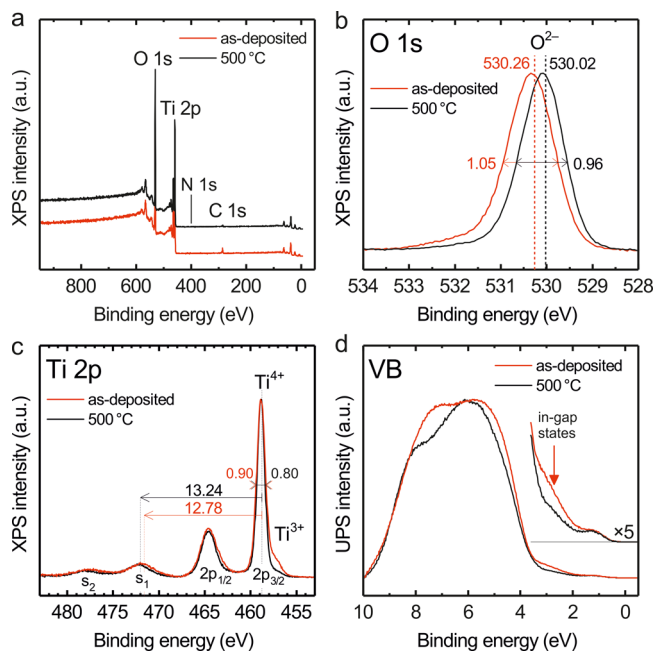


Figure 4. XP (a) survey spectra, (b) O 1s, (c) Ti 2p, and (d) UPS spectra of the valence band (VB) for the ALD-grown black TiO₂ film and 500 °C oxidized film.

The O 1s XPS peak is centered at 530 eV as expected for O²⁻ anions of the TiO₂ structure¹⁶ and the peak is slightly shifted to a lower binding energy upon oxidation (Figure 4b). This 0.2 eV shift and the decrease in the full width at half-maximum (fwhm) of the O 1s and Ti 2p XPS peaks take place gradually with increasing oxidation temperature (Figure S2) and are a result of the ordering of the amorphous phase to the crystalline rutile phase of TiO₂. We note that no such gradual change in neither Ti³⁺ concentration or in O/Ti ratio with temperature was observed (Figure S2a). The majority of Ti³⁺ was oxidized already at 200 °C and the O/Ti ratio was close to 2 throughout the temperature range.

The shakeup satellite peak originates from the excitation of a valence electron to a previously unoccupied state by the outgoing Ti 2p photoelectron according to the sudden approximation of photoemission.¹⁷ Thus, any change in the valence band structure, i.e. Ti–O bonding, may reflect to the charge transfer energy. Indeed, the UPS spectrum of the as-deposited sample (Figure 4d) reveals in-gap states at 2.5 eV that are efficiently removed upon oxidation treatments. Following the removal of in-gap states, the Ti 2p_{3/2} shakeup separation energy was observed to increase with oxidation temperature. The changes in the Ti–O bonding are also evident from the changes in the O 1s binding energy as pointed out above. Therefore, the in-gap states can be assigned to the lattice disorder¹⁸ and the subtle deviations in electronic structure compared to crystalline rutile TiO₂ presented above characterize the unique electronic structure of amorphous

ALD TiO₂. We note that the careful monitoring of the oxidation-treatment-induced changes in the electronic structure allowed the distinction between the doping,¹⁹ Ti^{2+/3+} defects,⁸ oxygen vacancies,²⁰ and the lattice-disorder-induced in-gap states.

The influence of oxidation on the performance of initially black TiO₂ as a photocatalyst for H₂O oxidation was studied as shown in Figure 5 and Figure S3. In accordance with our

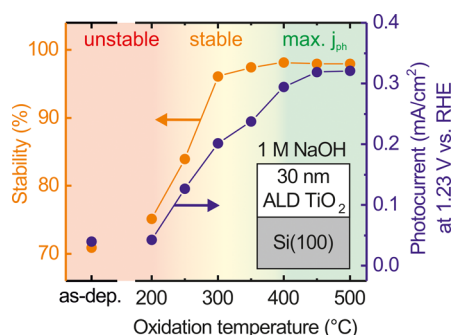


Figure 5. Photoelectrochemical stability and photocurrent (in 1 M NaOH) of the ALD grown, initially black, TiO₂ film after oxidation in temperature range from 200 to 500 °C.

previous work,⁸ the as-deposited black TiO₂ exhibits PEC instability and negligible photocurrent at 1.23 V vs RHE in 1 M NaOH. Only slight change in the PEC stability was observed upon oxidation at 200 °C followed by more dramatic change for increasing temperatures. Therefore, the oxidation of trapped charge carriers at 200 °C does not alone provide an explanation for the PEC stability nor for the increase in photocurrent with oxidation temperature. A reasonable stability is obtained after oxidation at 300 °C and above, whereas photocurrent continues to increase reaching saturation value for samples oxidized at >400 °C. The photocurrent was found to improve with the degree of TiO₂ crystallization and reach saturation for crystallized rutile TiO₂.

The improvement in PEC stability was found to correlate with crystallization, which supports earlier results that the stability of crystalline TiO₂ outperforms the amorphous phase.²¹ Albeit the complete crystallization of TiO₂ thin film required oxidation at >400 °C, the SEM images (Figure 3a) show that the surface is mostly crystallized already at 300 °C. Thus, the crystallized surface alone is sufficient requirement to endow improved PEC stability to the TiO₂ thin film. Although am-TiO₂ has been shown to both experimentally and theoretically exhibit several orders of magnitude higher dissolution rates in 1 M NaOH than crystalline polymorphs,²² we emphasize that the stability of black am-TiO₂ can also be improved by controlling the defect distribution.⁸

The unique properties of disordered ALD-TiO₂ include controlling the Ti³⁺ self-doping via growth temperature and thermal modification of defect and crystal structure. Recently we showed that annealing in UHV results in increase in Ti³⁺ states in the film and promotes PEC stability via the formation of O⁻.⁸ The facile modification treatments manifest the diversity of ALD-TiO₂ in applications ranging from conductive interlayers, to electrically leaky protection layers and photocatalyst materials.

In the present study, we have shown that black TiO₂ with enhanced absorbance in the wavelength range of 400–800 nm can be deposited as a conformal amorphous thin film using

ALD. We have demonstrated that the physicochemical properties of TiO₂ can be controlled by postannealing treatments either in reductive or oxidative conditions. The black as-deposited TiO₂ shows exceptionally high electrical conductivity of 150 S/m, but suffers from poor PEC stability and dissolves in alkaline conditions. Annealing treatment in extremely reductive conditions (UHV) at 500 °C transforms the black as-deposited TiO₂ into a photoelectrochemically stable phase of black TiO₂ retaining its amorphous structure.⁸ On the other hand, oxidation in air at 500 °C crystallizes TiO₂ into rutile phase with the maximum efficiency as photocatalyst for photoelectrochemical H₂O oxidation. The unprecedented diversity of ALD-TiO₂ can be rationalized by the propensity of the molecular structure toward local changes in the bonding configuration that affects the charge carrier densities via modified electronic structure. This unfolds the tremendous optoelectronic properties of TiO₂.

■ ASSOCIATED CONTENT

Supporting Information

The Supporting Information is available free of charge on the ACS Publications website at DOI: 10.1021/acsami.8b20608.

UV–vis absorption, XPS, PEC data as a function of oxidation temperature, and experimental details (PDF)

■ AUTHOR INFORMATION

Corresponding Author

*Email: Harri.Ali-Loytty@tut.fi.

ORCID

Harri Ali-Löyty: 0000-0001-8746-7268

Markku Hannula: 0000-0003-1110-7439

Kimmo Lahtonen: 0000-0002-8138-7918

Present Address

Surface Science Group, Laboratory of Photonics, Tampere University of Technology, P.O. Box 692, FI-33101 Tampere, Finland

Notes

The authors declare no competing financial interest.

■ ACKNOWLEDGMENTS

This work was supported by the Academy of Finland (decision numbers 141481, 286713 and 309920). H.A. and B.D.B. were supported by the Jenny and Antti Wihuri Foundation. M.H. was supported by the TUT's Graduate School and Emil Aaltonen Foundation.

■ REFERENCES

- (1) Liu, X.; Zhu, G.; Wang, X.; Yuan, X.; Lin, T.; Huang, F. Progress in Black Titania: A New Material for Advanced Photocatalysis. *Adv. Energy Mater.* **2016**, *6* (17), 1385–1388.
- (2) Selcuk, S.; Zhao, X.; Selloni, A. Structural Evolution of Titanium Dioxide during Reduction in High-Pressure Hydrogen. *Nat. Mater.* **2018**, *17* (10), 923–928.
- (3) Wang, B.; Shen, S.; Mao, S. S. Black TiO₂ for Solar Hydrogen Conversion. *J. Mater. Chem.* **2017**, *3* (2), 96–111.
- (4) Yan, X.; Li, Y.; Xia, T. Black Titanium Dioxide Nanomaterials in Photocatalysis. *Int. J. Photoenergy* **2017**, *2017*, No. 8529851.
- (5) Hu, S.; Shaner, M. R.; Beardslee, J. A.; Lichterman, M.; Brunschwig, B. S.; Lewis, N. S. Amorphous TiO₂ Coatings Stabilize Si, GaAs, and GaP Photoanodes for Efficient Water Oxidation. *Science* **2014**, *344* (6187), 1005–1009.

(6) Sivula, K. Defects Give New Life to an Old Material: Electronically Leaky Titania as a Photoanode Protection Layer. *ChemCatChem* **2014**, *6* (10), 2796–2797.

(7) Yu, Y.; Sun, C.; Yin, X.; Li, J.; Cao, S.; Zhang, C.; Voyles, P. M.; Wang, X. Metastable Intermediates in Amorphous Titanium Oxide: A Hidden Role Leading to Ultra-Stable Photoanode Protection. *Nano Lett.* **2018**, *18* (8), 5335–5342.

(8) Hannula, M.; Ali-Löytty, H.; Lahtonen, K.; Sarlin, E.; Saari, J.; Valden, M. Improved Stability of ALD Grown Amorphous TiO₂ Photoelectrode Coatings by Thermally Induced Oxygen Defects. *Chem. Mater.* **2018**, *30* (4), 1199–1208.

(9) Yang, Y.; Ling, Y.; Wang, G.; Liu, T.; Wang, F.; Zhai, T.; Tong, Y.; Li, Y. Photohole Induced Corrosion of Titanium Dioxide: Mechanism and Solutions. *Nano Lett.* **2015**, *15* (10), 7051–7057.

(10) Di Valentin, C.; Pacchioni, G.; Selloni, A. Reduced and N-Type Doped TiO₂: Nature of Ti³⁺ Species. *J. Phys. Chem. C* **2009**, *113* (48), 20543–20552.

(11) Burstein, E. Anomalous Optical Absorption Limit in InSb. *Phys. Rev.* **1954**, *93* (3), 632–633.

(12) Yoshihara, T.; Katoh, R.; Furube, A.; Tamaki, Y.; Murai, M.; Hara, K.; Murata, S.; Arakawa, H.; Tachiya, M. Identification of Reactive Species in Photoexcited Nanocrystalline TiO₂ Films by Wide-Wavelength-Range (400–2500 Nm) Transient Absorption Spectroscopy. *J. Phys. Chem. B* **2004**, *108* (12), 3817–3823.

(13) Hanaor, D. A. H.; Sorrell, C. C. Review of the Anatase to Rutile Phase Transformation. *J. Mater. Sci.* **2011**, *46* (4), 855–874.

(14) Woicik, J. C.; Weiland, C.; Rumaiz, A. K. Loss for Photoemission versus Gain for Auger: Direct Experimental Evidence of Crystal-Field Splitting and Charge Transfer in Photoelectron Spectroscopy. *Phys. Rev. B: Condens. Matter Mater. Phys.* **2015**, *91* (20), 201412.

(15) Zuo, F.; Wang, L.; Wu, T.; Zhang, Z.; Borchardt, D.; Feng, P. Self-Doped Ti³⁺ Enhanced Photocatalyst for Hydrogen Production under Visible Light. *J. Am. Chem. Soc.* **2010**, *132* (34), 11856–11857.

(16) Naumkin, A. V.; Kraut-Vass, A.; J. C. P. *NIST XPS Database 20*, Version 4.0; National Institute of Standards and Technology, 2008.

(17) Hedin, L.; Lee, J. D. Sudden Approximation in Photoemission and Beyond. *J. Electron Spectrosc. Relat. Phenom.* **2002**, *124* (2), 289–315.

(18) Chen, X.; Liu, L.; Yu, P. Y.; Mao, S. S. Increasing Solar Absorption for Photocatalysis with Black Hydrogenated Titanium Dioxide Nanocrystals. *Science* **2011**, *331* (6018), 746–750.

(19) Asahi, R.; Morikawa, T.; Ohwaki, T.; Aoki, K.; Taga, Y. Visible-Light Photocatalysis in Nitrogen-Doped Titanium Oxides. *Science* **2001**, *293* (5528), 269–271.

(20) Guo, Z.; Ambrosio, F.; Pasquarello, A. Hole Diffusion across Leaky Amorphous TiO₂ Coating Layers for Catalytic Water Splitting at Photoanodes. *J. Mater. Chem. A* **2018**, *6* (25), 11804–11810.

(21) Ros, C.; Andreu, T.; Hernández-Alonso, M. D.; Penelas-Pérez, G.; Arbiol, J.; Morante, J. R. Charge Transfer Characterization of ALD-Grown TiO₂ Protective Layers in Silicon Photocathodes. *ACS Appl. Mater. Interfaces* **2017**, *9* (21), 17932–17941.

(22) Shkol'nikov, E. V. Thermodynamics of the Dissolution of Amorphous and Polymorphic TiO₂ Modifications in Acid and Alkaline Media. *Russ. J. Phys. Chem. A* **2016**, *90* (3), 567–571.